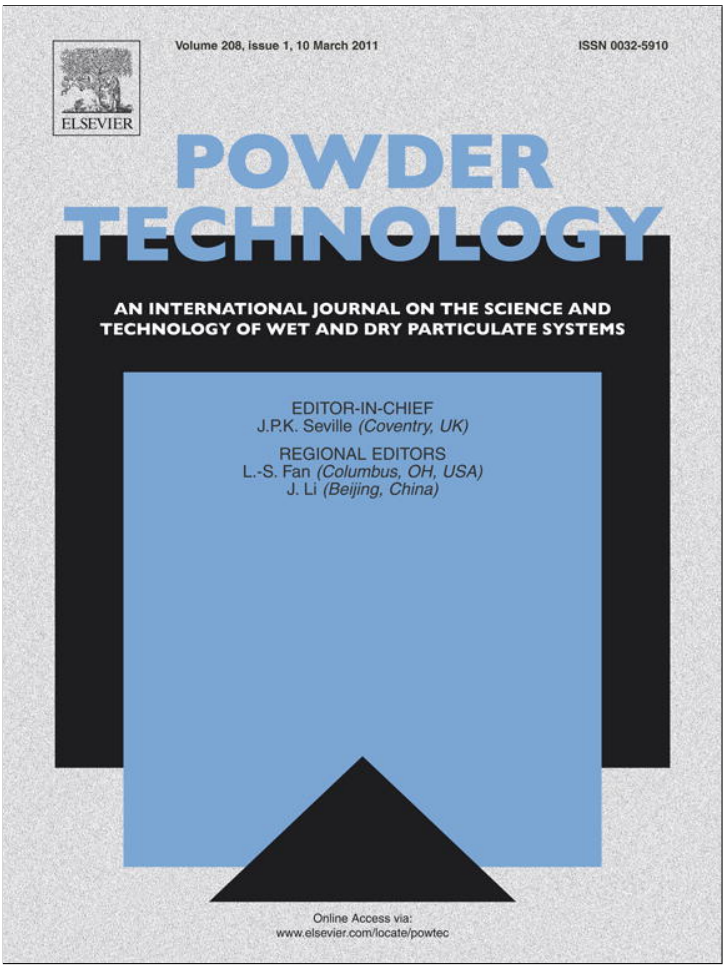

Powder Technology 208 (2011) 205–214

Contents lists available at ScienceDirect

Powder Technology

journal homepage: www.elsevier.com/locate/powtec

Influence of spray-drying operating conditions on *Rhamnus purshiana* (Cáscara sagrada) extract powder physical properties

Loreana Gallo [b], Juan M. Llabot [a], Daniel Allemandi [a], Verónica Bucalá [b], Juliana Piña [b,*]

[a] Department of Pharmacy, Facultad de Ciencias Químicas, Universidad Nacional de Córdoba, CONICET, Edificio de Ciencias II, Ciudad Universitaria, (5000) Córdoba, Argentina
[b] Department of Chemical Engineering – PLAPIQUI – Universidad Nacional del Sur – CONICET Camino La Carrindanga Km. 7, (8000) Bahía Blanca, Argentina

ARTICLE INFO

Article history:
Received 15 February 2010
Received in revised form 9 November 2010
Accepted 18 December 2010
Available online 24 December 2010

Keywords:
Rhamnus purshiana
Cáscara sagrada
Dry plant extract
Spray-drying
Factorial design
Direct compression

ABSTRACT

The aim of this work was to study *Rhamnus purshiana* (Cáscara sagrada) extract spray-drying in order to obtain powders with good rheological properties for direct compression (DC) and stability attributes.
The experiments were carried out in a Büchi B-290 Mini Spray Dryer using colloidal silicon dioxide as carrier agent. A 2^{5-1} fractional factorial statistical design was used to find adequate spray-drying operating conditions to produce Cáscara sagrada powders with good flow, good compactability properties, high process yield, low moisture content, low hygroscopicity, and caking tendency. Morphology, size, structural and thermal properties of the particles were also evaluated. The operating variables studied were air inlet temperature, atomization air flow rate, pump feed rate, aspiration capacity, and feed solids concentration.
The 2^{5-1} factorial experimental design used was a good strategy to establish spray-drying operating conditions to produce Cáscara sagrada extract powders with good properties for direct compression and high process yields. Colloidal silicon dioxide was an effective drying adjuvant. Its use in relatively high concentrations together with low atomization air flow rates improved powder flowability, increased the product's glass transition temperature, and decreased its moisture content and hygroscopicity.

1. Introduction

In the last few years, a marked increase in the use of the so-called "traditional medicine" has been observed [1]. This therapeutic strategy is based on the application of phytomedicines whose active components are constituted by vegetable drugs.

In particular *Rhamnus purshiana* (Rhamnaceae), commonly known as Cáscara sagrada, is frequently used due to its effective, economical, and natural laxative action [2]. This plant is indigenous to Southwestern Canada and the Pacific Northwest of the United States of America. The laxative effects of Cáscara sagrada are attributed to the presence of hydroxyanthracene glycosides in the plant bark. After oral administration, these compounds are not absorbed in the upper gastrointestinal tract; instead, they are passed – undigested – to the colon, where they are hydrolyzed by intestinal bacteria to form pharmacologically active metabolites. These metabolites, due to their stimulant and irritating properties, accelerate colonic transit [3].

Tablets are still the most frequently consumed dosage form because of manufacturing simplicity, administration convenience, accurate dosing and stability compared to oral liquids [4]. Direct compression (DC) is the preferred route for tablet preparation; it offers several advantages such as low labor costs, processing time, energy consumption, etc. [5].

In the specific case of phytomedicine tablets, the active ingredient is a dry plant extract composed of many substances that act synergically to produce the desired pharmacological effect [6]. Generally, dry plant extracts – including Cáscara sagrada – are hygroscopic and have poor rheological properties and compactability. For these reasons, they cannot be used for DC without prior addition of carriers and/or use of appropriate pre-processing technologies [7]. Therefore, the production of stable, dry plant extracts with good flow properties is a major challenge for both formulators and manufacturers in the phytomedicine and nutraceutical industries.

Continuous operations, like spray-drying, have been preferred over batch processes because of reduced time-to-market due to scale-up benefits and better product quality — no batch to batch variations, i.e. clinical trial and production batches are produced in the same equipment [8]. Nevertheless, spray-drying technology requires adequate adjustment of operating conditions as well as of the composition of feed solution — that contains the active principles. The operating variables for spray driers using binary nozzles are: inlet air temperature, atomization airflow, pump speed i.e. liquid flow rate-, aspirator suction velocity and solids concentration, and composition of the solution/dispersion to be spray-dried. Understanding how changes in these processing parameters affect rheological and stability properties in the powders produced is desirable for further industrial production of solid dosage forms by DC.

* Corresponding author. Tel.: +54 291 486 1700x265; fax: +54 291 486 1600.
E-mail address: julianap@plapiqui.edu.ar (J. Piña).

0032-5910/$ – see front matter © 2010 Elsevier B.V. All rights reserved.
doi:10.1016/j.powtec.2010.12.021

Stickiness of herbal extract powders on the unit walls is one of the most frequent problems encountered in spray-drying. Fluid plant extracts can be successfully dried with improvements in dryer design/operation, previous addition of carriers to plant extracts, or both [9]. Maltodextrin, cashew tree, and Arabic gums and colloidal silicon dioxide, among others, have been used to enhance plant extract spray-drying yields [10–12]. In particular, the use of colloidal silicon dioxide allows for production of non-hygroscopic dry plant extract, with good flowability, compressibility, and compactability properties [9,13–15]. Therefore, colloidal silicon dioxide appears as an interesting excipient for the formulation of dry extracts. Although this drying adjuvant has been recommended to produce dry plant extracts via spray-drying, the selection of spray-drier operating conditions and carrier concentration for Cáscara sagrada powder production cannot be directly inferred from other plant/carrier systems.

Based on the above reasons and considering the lack of scientific literature with regard to *R. purshiana* extract drying, the feasibility of spray-drying this plant extract using colloidal silicon dioxide as a drying aid is studied.

The main goal of this work is the production of Cáscara sagrada powders by means of spray-drying operations with high process yields, good rheological properties for DC and stability attributes. Since the number of process variables is relatively high – inlet air temperature and flow rate, atomization airflow, solution flow rate, and solids concentration –, a 2^{5-1} fractional factorial statistical design is selected to find the optimal set of spray-drier operating conditions that leads to high quality powders and process yields.

2. Materials and methods

2.1. Materials

The dried bark of Cáscara sagrada – European Pharmacopoeia name: *Rhamnus purshianus* D.C. – was used as received from the supplier (Droguería Argentina). The pieces of dried bark were slightly channeled or nearly flat, generally 1–5 mm thick, 10–30 mm long and up to 2 cm wide. The outer surface was brown and usually more or less covered by a whitish coat of lichens. The inner surface was light yellow to reddish-brown. The physical appearance of the dried bark used was in agreement with the description of various pharmacopoeias [3,16,17].

Colloidal silicon dioxide (Aerosil 200®, Degussa AG) was used as received from the supplier. Distilled water was used for preparation of fluid plant extracts and aqueous dispersions to be spray-dried.

2.2. Fluid plant extract (FPE) preparation

0.9 kg of Cáscara sagrada bark were weighted accurately and mixed with 4000 ml of boiling water. This mixture was macerated for 3 h and then transferred to a percolator. Extra boiling water, used as menstruum, was continuously poured into the percolator until 5000 ml of the fluid extract were collected [16].

Thin Layer Chromatography (TLC) was used to analyze the FPE and identify its active compounds, since cascarosides A and B represent a high proportion of total hydroxyanthracene glycosides [3,18–20]. TLC experimental conditions were selected according to the guidelines given by Wagner and Bladt [21]. Ethyl acetate:methanol:water (100:13.5:10) was used as solvent system and 20 μl of the FPE were spotted near the bottom of the TLC plate. The plate was sprayed with 10 ml of 10% ethanolic potassium hydroxide reagent and visualized under 365 nm UV.

Total hydroxyanthracene derivatives and cascarosides were quantified using 1 g of a spray-dried plant extract without carrier, following the method reported in USP 30-NF 25 [16].

2.3. Solid residue (SR) assay

The SR content of fluid plant extracts was determined by evaporation of the solvent under reduced pressure, followed by drying in an oven at 80 ºC to constant weight.

2.4. Spray-drying sample preparation

FPE and colloidal silicon dioxide were the ingredients used to prepare the dispersion to be spray-dried. The colloidal silicon dioxide: SR ratio was 0.5:1 and 1:1. A magnetic stirrer bar, rotating at 1000 rpm, was used for 30 min before dispersion atomization, so as to keep it homogenized.

2.5. Particle morphology and size distribution

Some selected spray-dried samples were dried under air flow on a porthole. Afterwards, these samples were metalized with gold in a PELCO 91000 sputter coater. Particle morphology was assessed in an EVO 40-XVP, LEO Scanning Electron Microscope (SEM).

Particle size distribution was measured using a laser light diffraction instrument, (Horiba LA-950 V2). Average particle size was expressed as *D [4,3]*, mean volume diameter.

2.6. Bulk and tap densities

In order to determine the density of spray-dried samples, the powder was gently poured into a 10 cm^3 graduate cylinder. Bulk density (D_B) was calculated as the ratio between the weight (g) of the sample contained in the cylinder and the volume occupied (10 cm^3).

Tap density (D_T) was estimated by tapping the cylinder until no measurable change in volume was noticed. Powder compressibility was evaluated using Carr's compressibility index (CI) [22] shown in Eq. (1):

$$CI = \frac{(D_T - D_B)}{D_T} 100 \quad (1)$$

2.7. Compactability curve

In order to study the compactability of selected spray-dried powders, materials were compressed in a hydraulic press with manometer (Delfabro) at different forces for 5 s. Flat punches with a 10.0 mm diameter were used. The hardness of each compact (150 mg) was determined as the average of 6 measurements using a hardness tester (Scout).

2.8. Angle of repose (α)

The angle of repose was determined by pouring a pre-defined mass of spray-dried powder through a funnel located at a fixed height on a graph paper flat horizontal surface and measuring the height (h) and radius (r) of the conical pile formed. The tangent of the angle of repose is given by the h/r ratio [23].

2.9. Moisture content (MC)

Powder moisture content was determined by a moisture analyzer with halogen heating (model M45, OHAUS). Sample moisture content analysis was performed immediately after the spray-drying step.

2.10. Hygroscopicity (HYG)

Hygroscopicity was determined by adapting the method proposed by Tonon et al. [11]. Spray-dried samples – approximately 0.2 g – were

stored in containers at 25 °C and 75.29% RH — given by a saturated aqueous solution of NaCl—. After 7 days, the samples were weighed. The hygroscopicity was expressed as g of adsorbed moisture per 100 g of dry solids. In addition, a change in the color of the spray-dried powders was observed.

2.11. Mixture viscosity

Viscosities of FPE and of mixtures of FPE with different colloidal silicon dioxide concentrations – colloidal silicon dioxide/SR equal to 0.5:1 and 1:1 – were measured. Measurements were taken in triplicate, at 20 °C using capillary viscometers – IVA 1 and 1B – immersed in a constant temperature bath.

2.12. Surface tension measurements

Surface tensions of FPE without carrier and of feed dispersions with 0.5:1 and 1:1 colloidal silicon dioxide:SR were measured using a Kruss Easy-Dyne tensiometer, K 20.

2.13. Thermal analysis. Tg determination

In order to study the glass transition temperature (T_g) of different spray-dried plant extracts, a differential scanning calorimeter (Pyris 1, Perkin Elmer) was used. Selected powder samples of 10 mg were placed in aluminum pans and scanned from 30 to 160 °C at a heating rate of 10 °C/min. The purpose of this first thermal scan was to eliminate the residual moisture that would interfere with spray-dried powder T_g determination. Then, the samples were cooled from 160 to 30 °C at a cooling rate of 10 °C/min and re-heated again from 30 to 160 °C at the same rate. T_g value was determined by the half ΔCp method [24].

2.14. X-ray diffraction (XRD)

XRD patterns were recorded using a Rigaku Geigerflek (DMAX 3 C) X-ray diffraction system. The anode X-ray tube was operated at 35 kV and 15 mA. Measurements were taken from 2° to 70° on the 2θ scale at a step size of 2°/min.

2.15. Process yield (PY)

The production yield was calculated as the ratio of the powder weight collected after every spray-drying experiment to the initial amount of solids in the sprayed dispersion volume.

2.16. Spray-drying and experimental design

The spray-drying process was performed in a laboratory-scale Mini Spray Dryer Büchi B-290 (Büchi Labortechnik AG). Technical data and a scheme of the drying apparatus can be found elsewhere [25]. A two fluid nozzle with a cap orifice diameter of 0.5 mm was used; the air atomizing pressure was kept constant at 6 bars for all the experiments.

A 2^{5-1} factorial experimental design was used to assess the effect of spray-drying operating variables on the powder properties. Five factors at two levels were considered: (A) drying air inlet temperature, (B) atomization air volumetric flow rate, (C) feed volumetric flow rate — expressed as % of the maximum pump rate-, (D) drying air volumetric flow rate – given as % of the maximum aspiration rate – and (E) feed solids concentration. Table 1 summarizes the levels of operating variables.

The dispersion concentrations studied were 5.59 (w/w) and 7.32% (w/w), with 0.5:1 and 1:1 colloidal silicon dioxide:SR ratios, respectively. Several authors have used the 1:1 ratio with colloidal silicon dioxide, such as, Souza and Oliveira [9], Takeuchi et al. [26], Bhaskar et al. [27] and Palma et al. [28], among others. The 0.5:1 ratio was selected to assess lower carrier content spray drying procedure feasibility.

Table 1
Process variables levels.

Parameter independent formulation	Low (−)	High (+)	Units
A (air inlet temperature)	130	170	°C
B (atomization air flow rate)	400	800	(l/h)
C (pump setting)	5	15	%
D (aspirator setting)	80	100	%
E (feed concentration)	5.59	7.32	% (w/w)

Regarding the highest adjuvant content, it is important to note that due to its safety characteristics [29] Aerosil 200 can be used as pharmaceutical carrier even in high proportions, with a very high lethal dose — LD50 in rats, oral administration equal to 3.16 g/kg.

Atomization air flow rate settings were the lowest (400 l/h) and highest (800 l/h) values recommended for the experimental unit [25]. 100% aspiration (about 35–38 m^3/h) was the highest setting attainable, while 80% (30–32 m^3/h) was the minimum feasible level to avoid dispersion condensation on the drying chamber surfaces. This last value was determined from several trial experiments. In order to ensure a constant drying air flow rate, the filter was replaced by a clean one after each experiment.

The 15% pump rate (3 ml/min) was set as the maximum feasible value because higher rates, even for different inlet air temperatures and aspiration levels, did not allow for water evaporation — i.e. some condensation on the dryer walls was observed. On the other hand, the lowest pump rate was fixed at 5% (1 ml/min) in order to process the total dispersion volume in reasonable time.

All the experimental runs were performed in randomized order and by duplicates to eliminate possible sources of bias [30,31]. The experiment design matrix is shown in Table 2. In this table, variable T_{out} represents the outlet air temperature.

The effects of operating variables on the responses: angle of repose, Carr's compressibility index, moisture content, hygroscopicity, outlet air temperature, process yield and mean volume diameter were studied. For some selected samples, particle morphology, structure and thermal properties were also evaluated.

The selected factorial experimental design is of resolution V, indicating that the main effects are confounded with four factors and that two-factor interactions are confounded with three-factor interactions [31]. Only main effects and two-factor interactions were considered by the statistical model. The statistical evaluation of the results was carried out by analysis of variance (ANOVA); the extent of the impact of each main factor as well as their two-factor interactions on the product properties was indicated by the F-value. The higher the F-value, the greater the factor impact on the response. Statistical significance was established through p-value; values lower than 0.05 indicate that the factor impact is significant with at least 95% confidence [32]. Responses were related to main effects and two-factor interactions by the following equation:

$$Y = b_0 + \sum_i b_i X_i + \sum_i \sum_{j>i} b_{ij} X_i X_j \quad (2)$$

where Y is the response or its mathematical transformation. The responses: angle of repose (α), Carr's Index (CI) and average particle size (D [4,3]) were mathematically transformed prior to statistical analysis because the experimental data for these responses did not follow normal distribution. The parameter b_0 is the interception — calculated as the arithmetic mean of the response for all the experiments-, b_i and b_{ij} are model coefficients for main effects and two-factor interactions, respectively. For main effects, a positive coefficient indicates that the response increases when the variable

Table 2
Experimental matrix according to 2^{5-1} factorial design and studied responses.

Run	A	B	C	D	E	α (°)[a]	CI (%)[b]	MC (%)[c]	HYG (g/100 g)[d]	T_{out} (°C)[e]	Y (%)[f]	*D [4,3]* (μm)[g]
1	−	+	−	+	+	35 ± 3	18.68 ± 1.23	2.70 ± 0.07	8.88 ± 0.34	65 ± 2.12	82.63 ± 0.74	9.13 ± 0.48
2	+	−	−	+	+	28 ± 3	19.74 ± 2.87	2.41 ± 0.08	7.89 ± 1.35	96 ± 2.12	82.00 ± 0.57	13.06 ± 0.48
3	−	+	−	−	−	31 ± 3	22.42 ± 1.79	3.64 ± 0.13	10.69 ± 0.89	49 ± 0.71	68.05 ± 0.49	8.30 ± 0.71
4	−	−	−	+	−	29 ± 2	21.74 ± 1.36	2.83 ± 0.30	11.35 ± 0.59	66 ± 1.41	79.00 ± 5.09	11.75 ± 0.26
5	+	+	−	−	+	31 ± 2	19.26 ± 3.72	2.75 ± 0.02	4.69 ± 2.04	72 ± 0.71	84.55 ± 0.07	9.52 ± 0.44
6	+	−	+	−	+	28 ± 2	20.70 ± 2.42	3.02 ± 0.08	9.91 ± 1.13	77 ± 0.71	69.87 ± 9.86	14.43 ± 0.85
7	−	−	−	−	+	28 ± 2	20.19 ± 3.05	3.01 ± 0.19	8.64 ± 0.64	74 ± 1.41	69.52 ± 9.79	13.41 ± 0.60
8	+	−	+	+	−	33 ± 3	24.04 ± 2.39	3.37 ± 0.19	10.77 ± 0.67	86 ± 3.54	77.85 ± 7.00	12.70 ± 0.89
9	+	−	−	−	−	33 ± 2	21.50 ± 3.34	3.62 ± 0.00	10.52 ± 0.82	86 ± 4.24	77.10 ± 0.62	12.99 ± 0.37
10	−	+	+	−	+	34 ± 2	16.84 ± 2.70	3.79 ± 0.16	7.81 ± 0.64	44 ± 1.41	70.99 ± 11.43	10.73 ± 1.62
11	+	+	−	+	−	35 ± 2	27.04 ± 2.11	4.71 ± 0.06	10.56 ± 0.93	63 ± 2.12	83.43 ± 2.59	8.84 ± 0.49
12	−	+	+	+	−	36 ± 4	28.23 ± 2.78	4.72 ± 0.28	11.53 ± 1.45	63 ± 2.83	77.28 ± 2.60	7.94 ± 0.08
13	−	−	+	−	−	31 ± 1	22.61 ± 3.14	4.30 ± 0.14	8.65 ± 0.04	65 ± 0.71	55.45 ± 1.48	12.17 ± 0.96
14	+	+	+	+	+	30 ± 2	18.31 ± 2.63	3.76 ± 0.01	9.92 ± 0.81	80 ± 0.71	85.70 ± 4.38	10.46 ± 1.45
15	+	+	+	−	−	35 ± 2	21.44 ± 2.43	4.25 ± 0.49	9.23 ± 0.61	65 ± 2.12	64.82 ± 3.85	8.58 ± 0.21
16	−	−	+	+	+	27 ± 2	20.03 ± 3.08	4.23 ± 0.10	10.63 ± 0.82	55 ± 0.00	67.38 ± 5.20	13.04 ± 0.41

[a] The values represent the mean of twenty determinations ± standard deviation.
[b] The values represent the mean of sixteen determinations ± standard deviation.
[c] The values represent the mean of two determinations ± standard deviation.
[d] The values represent the mean of four determinations ± standard deviation.
[e] The values represent the mean of two determinations ± standard deviation.
[f] The values represent the mean of two determinations ± standard deviation.
[g] The values represent the mean of twelve determinations ± standard deviation.

level increases while a negative coefficient shows that the response increases when the variable level decreases. X_i represents the level of the factors studied (A to E, see Table 1) in coded form — i.e. +1 and −1 for the highest and lowest levels respectively. Arithmetic mean and model coefficients for main effects and two-factor interactions as well as R^2 coefficient values are reported in Table 3.

3. Results and discussion

3.1. Plant extract characterization

The fluid plant extract SR value, measured in triplicate, was 3.80 ± 0.12% (w/v).

TLC analysis showed two yellow bands with retention times around 0.05 and 0.14, these values are in agreement with retention times reported by Wagner and Bladt [21], for cascarosides A and B, respectively, and the same experimental conditions. Besides, other yellow bands with retention times of 0.2 and 0.24, representative of cascarosides C and D, were found. The results confirm the presence of cascarosides A, B, C, and D; compounds known as active components.

Quantitative determination showed that 1 g of the spray-dried extract contained 232 mg of hydroxyanthracene derivatives and 180 mg of cascarosides, i.e. a total amount of active components of 41.2% (w/w). The recommended dose for adults and children 12 years of age and over is 20–30 mg of hydroxyanthracene glycosides per day [3,33–35]. Therefore, the daily DPE intake – without carrier – would be around 73 mg.

3.2. Statistical evaluation of the experimental design

3.2.1. Angle of repose

Flow properties of dried products are directly related to their behavior during storage, handling, and processing [23]. According to USP 30-NF 25 [16], for repose angles between 25–30° powder flow is excellent, among 31–35° the flow is good and within the range 36–40° the flow is fair. For values higher than 41°, the powder has bad flow properties.

As shown in Table 2, the best angle of repose was shown by the powder obtained from test 16 (α = 27 ± 2°), whose flow can be considered excellent. Besides, the powders obtained from

Table 3
Coefficients of significant main effects and two-factor interactions (Eq. (2)).

Model coeff.	$Y^a = \alpha^{-2.52}$	Model coeff.	$Y^a = CI^3$	Model coeff.	$Y = MC$	Model coeff.	$Y = HYG$	Model coeff.	$Y = T_{out}$	Model coeff.	$Y = PY$	Model coeff.	$Y^a = D[4,3]^{-1}$
b_0	1.74E−4	b_0	10390.35	b_0	3.58	b_0	9.48	b_0	68.81	b_0	74.71	b_0	0.094
b_B	−2.68E−5	b_E	−2978.01	b_E	−0.37	b_E	−0.93	b_A	8.88	b_D	4.68	b_B	0.016
b_E	2.01E−5	b_{DE}	−1682.21	b_C	0.35	b_D	0.71	b_B	−6.56	b_C	−3.56	b_E	−6.07E−3
b_{AE}	1.24E−5	b_D	1679.61	b_{AC}	−0.26	b_{CE}	0.69	b_{CE}	−4.06	b_A	3.44	b_{BE}	−2.80E−3
b_{AB}	1.06E−5	b_{BD}	1549.69	b_B	0.21	b_{AC}	0.45	b_{BC}	2.75	b_B	2.45	b_{CE}[b]	−2.00E−3
b_{CE}	1.01E−5	b_{BE}	−1319.07	b_{BD}	0.17	b_{BE}	−0.41	b_D	2.62	b_{BE}	1.93	b_A[b]	−2.3E−3
b_{BE}	−9.95E−6	b_{AC}	−1310.44	b_{BE}	−0.17	b_{BD}	0.35	b_{BD}	2.50	b_E	1.85	b_{AD}[b]	−1.75E−3
b_{BD}	−8.19E−6	b_{CD}	748.85	b_{AE}	−0.15	b_C	0.33	b_C	−2.25	b_{DE}	−1.83	b_D[b]	1.34E−3
b_{DE}[b]	4.24E−6	b_{BC}	−705.43	b_{AB}	0.15	b_B[b]	−0.31	b_{AE}	1.81	b_{CD}[b]	1.20	b_{CE}[b]	−2.32E−3
b_A[b]	−3.62E−6	b_{AB}[b]	−557.52	b_{CE}	0.14	b_A[b]	−0.29	b_{AB}	−1.63	b_{BC}[b]	1.07	b_{AE}[b]	1.19E−3
b_{CD}[b]	−3.62E−6	b_{AE}[b]	489.22	b_{CD}	0.08	b_{AB}[b]	−0.27	b_{CD}	1.56	b_{AB}[b]	−0.99	b_{BC}[b]	−6.15E−4
b_{BC}[b]	−3.51E−6	b_B[b]	376.33	b_A[b]	−0.07	b_{CD}[b]	0.19	b_{BE}[b]	1.37	b_{AD}[b]	−0.60	b_{DE}[b]	4.40E−4
b_{AC}[b]	2.56E−6	b_{CE}[b]	−341.88	b_{DE}[b]	0.06	b_{AE}[b]	−0.15	b_E[b]	1.25			b_{BD}[b]	−3.86E−4
b_D[b]	−2.24E−6	b_A[b]	−181.17	b_{AD}[b]	0.04			b_{AC}[b]	1.06			b_{CD}[b]	3.77E−4
b_C[b]	−3.91E−7	b_C[b]	6.62	b_D[b]	0.01			b_{DE}[b]	0.94			b_{AB}[b]	−1.99E−4
R^2	0.96	R^2	0.94	R^2	0.97	R^2	0.85	R^2	0.99	R^2	0.81	R^2	0.94

[a] Mathematically transformed responses.
[b] Not significant.

experiments 2, 4, 6 and 7 also presented angles of repose lower than 30°, and, thus, excellent flowability.

The ANOVA analysis indicated that the most significant main factors affecting the angle of repose were atomization air flow rate (B) and solids concentration (E), with F-values of 176.14 ($p<0.0001$) and 99.08 ($p<0.0001$), respectively (Fig. 1a). According to the coefficients given in Table 3, the angle of repose was improved when the atomization air flow rate was decreased and the solids concentration was increased. Both actions led to bigger particles due to greater droplet sizes with higher solids content.

The effect of solids concentration on the angle of repose is in agreement with the results reported by Moreira et al. [12] for acerola pomace extract using maltodextrin-cashew tree mixtures as carriers. These authors also found that inlet air temperature (between 170 and 200 °C) had influence on the angle of repose. In fact, the angle of repose increased as the inlet temperature was risen due to decreases in product humidity and hygroscopicity.

Although in this work inlet air temperature was not found as a significant main effect, its interactions with solids concentration (AE) and atomization air flow rate (AB) were important ($p<0.0001$ and F-values of 37.52 and 27.71, respectively). The inlet air temperature lower impact observed on the angle of repose may be attributed to the use of colloidal silicon dioxide, a carrier that led to dried samples with moisture contents lower than those reported by Moreira et al. [12], even for the lowest inlet temperature used in the experiments presented here.

3.2.2. Compressibility and compactability

Carr's compressibility indexes of 10% indicate excellent flow, between 11% and 15% they indicate good flowability, between 16% and 20% the powder flow is fair, between 21% and 25% the product has acceptable flow properties and between 26% and 31% the powder flow is poor [16].

According to Table 2, the lowest *CI* (16.84 ± 2.70%) was shown in sample 10 with a fair flow. Samples 1, 2, 5, 6, 7, 10, 14, and 16 also showed fair flow with *CI* values between 16.84 ± 2.70 and 20.70 ± 2.42%. For most samples, a relative agreement between the *CI* and α measurement was found. Therefore, several manufactured spray-dried powders had appropriate properties for DC.

As for the α response, the greatest impact factor on *CI* was the feed solids concentration (E) with an F-value of 98.86 ($p<0.0001$) (Fig. 1b). The highest solids concentration led to the lowest Carr's compressibility index, as can be inferred from the sign of the corresponding coefficient in Table 3.

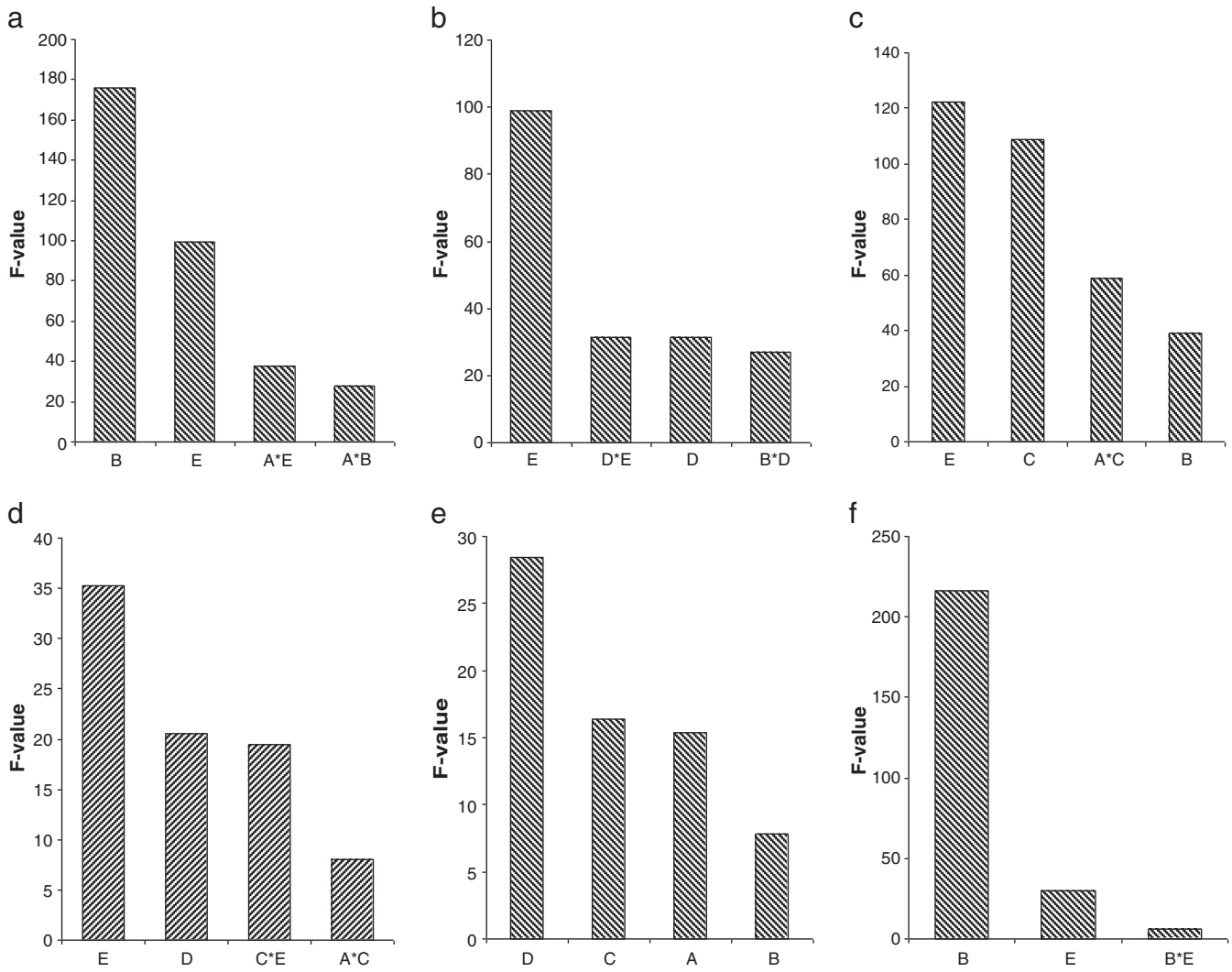

Fig. 1. F-values of significant main effects and two-factor interactions with *p*-values lower than 0.0001 on the responses: a) angle of repose, b) Carr's compressibility index, c) moisture content, d) hygroscopicity, e) process yield and f) mean volume size.

This response showed six significant two-factor interactions, being the solids concentration drying air flow rate (DE) and the atomization-aspiration flow rates (BD) the more relevant ones — $p<0.0001$, F-values 31.55 and 26.77, respectively. The aspiration rate also influenced Carr's index with the same order of importance as the afore-mentioned two-factor interactions — F-value 31.45, $p<0.0001$.

Samples 12 – poor powder flow – and 16 – good-fair powder flow – were subject to compression tests. Fig. 2 presents the compact hardness for both powders as a function of compression force. For all compression forces tested, the compact hardness corresponding to sample 16 – even for low compression forces – was above 4 kg, usually considered to be the minimum for satisfactory tablets [36]. However, sample 12 required compression forces higher than 10 kN to give compacts with adequate hardness. These results demonstrate that sample 16, corresponding to the powder with the best angle of repose and a fair Carr's index, had better compactability properties than sample 12, representing the powder with the worst angle of repose and Carr's index.

3.2.3. Moisture content

The moisture content was in the range of 2.41 ± 0.08 and 4.72 ± 0.28 wt.% (Table 2). The main factors that most affected this response were feed solids concentration (E) and pump setting (C), with F-values of 122.59 ($p<0.0001$) and 108.97 ($p<0.0001$), respectively (Fig. 1c).

The sign of the coefficient that relates *MC* to solids concentration was negative (see Table 3), indicating that higher solid concentrations produced powders with lower moisture contents. This behavior is in agreement with previous work on plant extract spray-drying with colloidal silicon dioxide [15]. On the other hand, as shown in Table 3, the use of higher feed flow rates (C) gave more moist powders due to higher water loads for evaporation. The effect observed for the pump rate on *MC* is particularly in agreement with the results reported by Tonon et al. [11] for spray-drying of açai (a fruit juice) using maltodextrin as carrier and also with many other spray-drying studies [30, 37].

The significant main effects E and C were involved in many significant two-factor interactions as revealed by the analysis of variance (Table 3). The most important two-factor interaction was the inlet air temperature-feed flow rate (AC) — F-value 59.02, $p<0.0001$. In different plant extract spray-drying with other carriers [11,30,38], the inlet air temperature appeared as one of the operating variables with more impact on *MC*. In those cases, higher inlet thermal levels led to lower powder moisture contents. Nevertheless, for *Schinus terebinthifolius* Raddi – plant extract – spray-drying with high concentrations of Aerosil 200 as drying adjuvant, Vasconcelos et al. [15] found that the inlet temperature did not affect powder residual moisture content.

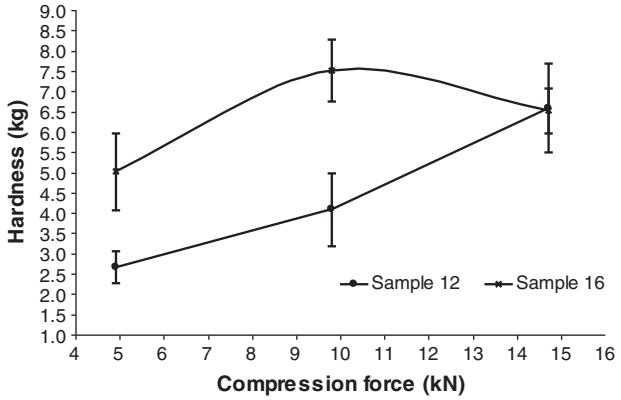

Fig. 2. Compactability curves for samples 12 and 16.

3.2.4. Powders hygroscopicity

Hygroscopicity values were between 4.69 ± 2.04 and 11.53 ± 1.45 g per 100 g of dry solids. Feed solids concentration – F-value 35.28, $p<0.0001$ – was the variable that most affected powder hygroscopicity (Fig. 1d). The lowest values were obtained for the highest Aerosil concentrations tested (Fig. 1d). This confirmed Aerosil's efficiency as a carrier agent, since its use in relatively high concentrations improved the angle of repose, Carr's index, powder moisture content, and hygroscopicity simultaneously. Moreover, samples 3, 4, 8, 9, 11, and 12 – corresponding to the lower Aerosil concentration – showed caking and color change from light yellow to dark brown — i.e. to the FPE natural color- after the conditioning performed to evaluate hygroscopicity. Color changes of spray-dried plant extracts during hygroscopicity testing have been also reported by Souza and Oliveira [9] for mixtures of *Bauhinia forficata* extract and for different concentrations of colloidal silicon dioxide. Aerosil is a white powder, which acts as color diluent for samples containing the highest value of Aerosil concentration. Besides, using maltodextrin, Quek et al. [38] observed loss of red-orange color in spray-dried watermelon powder as the concentration of the excipient was increased.

As it will be shown in Section 4.3., the higher the feed Aerosil content the more rounded and smoother the shape and surface of dried particles are. On the other hand, for lower Aerosil concentrations, the particles have shown a shriveled surface similar to the morphological structure of the dried plant extract without colloidal silicon dioxide. Even though Aerosil was able to hold substantial quantities of liquid within the interstitial volume of its agglomerates, for the samples with low solids concentration the amount of carrier available did not seem to be enough to totally confine the plant extract within the agglomerates' interstitial volume. For high Aerosil concentrations, the plant extract could be trapped within these solid particles and then it could be almost unavailable for water adsorption. This result would be in agreement with the high hygroscopicity shown by the dried plant extract (DPE), obtained without any drying adjuvant and at the same operating conditions as experimental run 16, which was 16.82 ± 0.42 g absorbed water/100 g powder. Moreover, after the conditioning at RH = 75% the DPE changed from dry powder to rubbery form.

Tonon et al. [11] evaluated the hygroscopicity of spray-dried açai powder at the same RH used in the present work, obtaining values between 12 and 15 g absorbed water/100 g powder. According to the results of the present work, the authors reported lower hygroscopicity values for higher carrier (maltodextrin) concentrations.

The second factor of importance on hygroscopicity was aspiration (D) — F-value 20.51, *p:* 0.0002-, higher aspirator levels gave higher hygroscopic powders. The main significant effect E was also involved in the most important two-factor interaction CE – pump setting – feed solids concentration, F-value 19.44, *p:* 0.0003.

3.2.5. Outlet temperature

As expected, the spray-drying process outlet temperature was influenced by several operating variables. In this study, the outlet temperature typically varied between 44 ± 1.41 and 96 ± 2.12 °C.

This response was primarily dictated by inlet temperature (A) — F-value 602.44, $p<0.0001$-; unsurprisingly higher inlet temperatures led to higher outlet temperatures. The second parameter with a significant influence on outlet temperature was the atomization air flow rate (B) — F-value 329.39, $p<0.0001$.

Based on an experimental factorial design, Tajber et al. [31] analyzed the spray-drying of a budesonide/formoterol solution. They found that outlet temperature was mainly affected – listed according to significance level – by pump setting, aspiration capacity,

Table 4
Viscosity and surface tension measurements.

Feed solution	Viscosity, cP	Surface tension, mN/m
FPE	2.47 ± 0.001	39.4 ± 0.1
FPE with 0.5:1 colloidal silicon dioxide:SR ratio	2.80 ± 0.002	42.4 ± 0.1
FPE with 1:1 colloidal silicon dioxide:SR ratio	10.31 ± 0.006	44.4 ± 0.1

SEM microphotographs of some selected *Rhamnus purshiana* (Cáscara sagrada) spray dried samples.

atomization air flow rate, and inlet air temperature. These authors used a wider range of solution feed flow rates (10–40%) than the one used in this work. This is the reason why, in the present work, pump setting did not appear as one of the more important main significant factors on T_{out}. Nonetheless, this variable was involved in the two most significant two-factor interactions — CE and BC. Tajber et al. [31] used aspiration levels between 70 and 100%, while in this work, the drying flow rate varied in the range of 80–100%. Finally, the authors used inlet temperatures between 78 and 84 °C, a low variation in comparison with the thermal levels chosen for this work (130–170 °C). Consequently, the degree of influence of operating variables appears to be dependent on the lower and upper levels selected for the experimental factorial design.

3.2.6. Process yield

Table 2 shows the yields achieved for each experiment. The lowest yield was for sample 13 (55.45 ± 1.48%) while the highest one was for sample 14 (85.70 ± 4.38%). Except in just a few experiments, the yields were greater than or equal to 70% being this value more than acceptable for lab-scale spray dryers.

The most significant main factor on the spray-drying yield was the percentage of aspiration (D), — F-value 28.42, $p<0.0001$. This variable was followed by feed solution flow rate – C, F-value 16.41, p: 0.0006 – and inlet air temperature – A, F-value 15.33, p: 0.0009 – (Fig. 1e). Higher aspirations, that led to a better separation rate in the cyclone, higher thermal levels in the spray chamber, and higher drag forces, improve the process yield. On the other hand, for lower pump rates water loading was almost completely evaporated decreasing the probability of dispersion condensation on the chamber walls and thus giving better process yields. Similarly, higher inlet temperatures made water evaporation easier. All significant main effects and two-factor interactions on *PY* are reported in Table 3.

Tonon et al. [11] also found that feed solution rate and inlet air temperature were significant effects on the process yield when spray-drying *Euterpe oleraceae* extract. On the other hand, Ståhl et al. [30] observed that aspiration was the effect with the greatest impact on the yield of a spray-dried insulin solution.

3.2.7. Mean particle size

All the samples showed unimodal particle size distributions, being the mean volume particle diameter values between 7.94 ± 0.08 and 14.43 ± 0.85 μm. Atomization air flow rate (B) – F-value 216.33, $p<0.0001$ – was the variable that most affected this response (Fig. 1f). The higher mean particle size was obtained for the lower atomization air flow rate level due to the bigger drops sprayed.

The second factor of importance was solids concentration (E) – F-value 30.11, $p<0.0001$ – that is highly related to feed solution viscosity and surface tension. Table 4 shows viscosity and surface tension values measured for the fluid extract without carrier and feed dispersions with 0.5:1 and 1:1 colloidal silicon dioxide:SR ratios. Dispersions with the highest solids concentrations showed the highest viscosity and surface tension values and also the biggest particles. This result is in agreement with the influence of viscosity and surface tension on solution droplet size, i.e. the higher the viscosity and surface tension the higher the drop size and, consequently, the mean particle volume [39]. Tonon et al. [11] found similar results in açai (*Euterpe oleraceae*) spray-drying with maltodextrin as carrier agent. These authors observed that higher liquid viscosity led to bigger droplets and, thus, to larger particles.

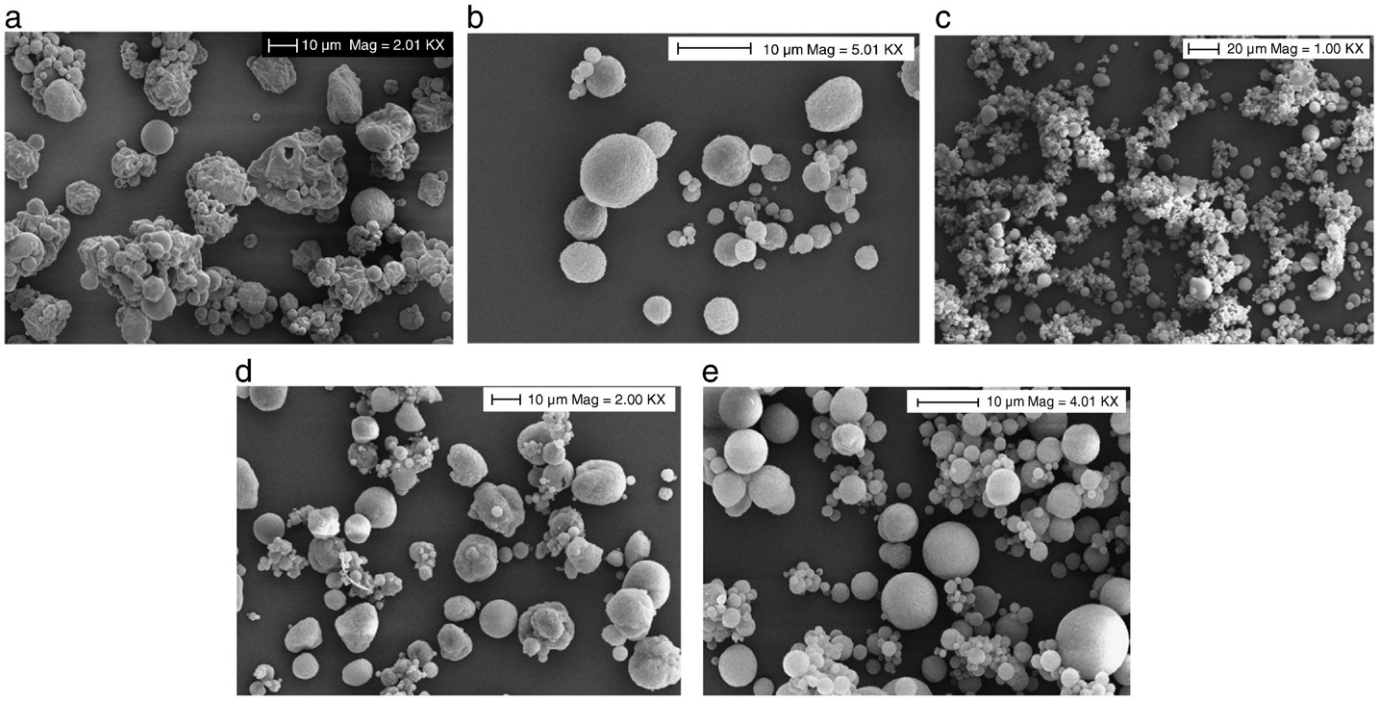

Fig. 3. SEM microphotographs. a) DPE, b) sample 16, c) sample 12, d) sample 8 and e) sample 1.

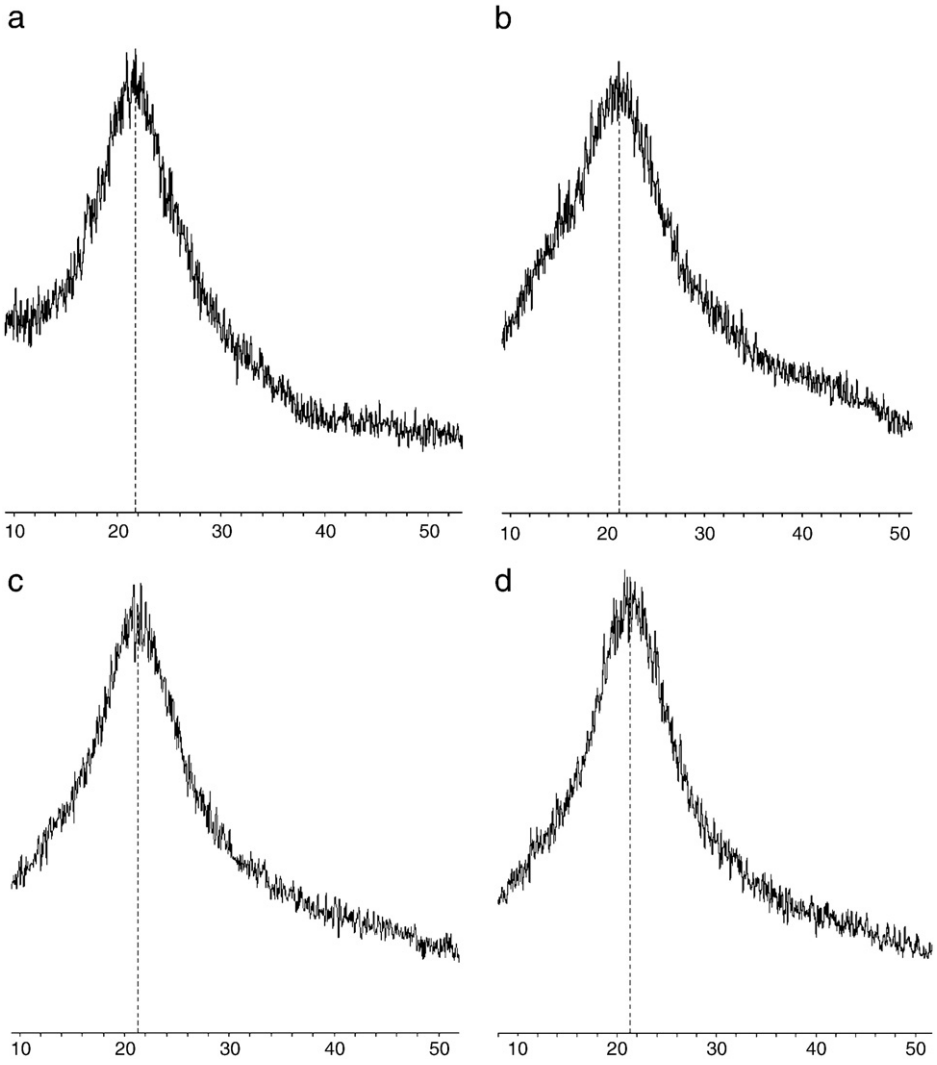

Fig. 4. PXRD patterns. a) DPE, b) colloidal silicon dioxide, c) sample 16 and d) sample 12.

Tajber et al. [31] also found that atomization airflow and solids feed concentration were significant main effects on mean particle size.

3.2.8. Particle morphology

Particle morphology was studied for samples 1, 8, 12, and 16 and for the DPE obtained at the same operating conditions as in experimental run 16.

DPE particles (Fig. 3a) showed shriveled surfaces and irregular shapes, as expected for natural extracts [40]. Sample 16, with the best powder flowability, showed relatively big spherical particles with smooth surfaces (Fig. 3b). In contrast, sample 12 – corresponding to the test with the worst powder flowability – presented a great amount of agglomerates (Fig. 3c) and particles with different surface patterns — some were smooth and others were shriveled like the dried plant extract without carrier. This sample showed the highest *MC* and hygroscopicity and the lowest *D [4,3]*, properties that promote particle agglomeration. Although sample 16 also had relatively high *MC* and hygroscopicity, coalescence phenomenon was not important probably because particles were bigger, smoother, and more spherical than those in sample 12.

Even though the mean size of sample 8 particles (Fig. 3d) was similar to that of sample 16, flowability properties – α and *CI* – were worse. Lower feed solids concentrations led to more irregular and shriveled particles, being these two morphological properties responsible for poor powder flowability in sample 8.

Both samples 1 (Fig. 3e) and 12, that presented different surface morphology — caused by variations in solids concentration, showed relatively fair powder flow. This result indicates that surface characteristics play a less important role on powder flowability than mean particle diameter [41]. In fact, when angles of repose were

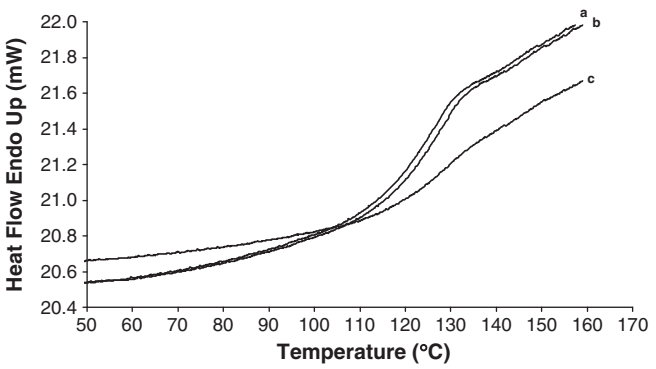

Fig. 5. DSC thermograms showing glass transition temperature. a) Sample 12, b) DPE and c) sample 1.

correlated to mean volume diameters, a linear decreasing trend was observed.

3.2.9. Powder X-ray diffraction (PXRD)

XRD measurements were taken for the DPE, the colloidal silicon dioxide and samples 16 and 12 that are representatives of good and bad powder flowability, respectively.

All the samples tested revealed a completely amorphous state, as it can be confirmed by the presence of broad non-defined peaks with abundant noises (Fig. 4) [42].

3.2.10. Thermal analysis. Tg determination

Amorphous products are metastable and vulnerable to caking or collapsing during storage. The stability of these products is forcefully associated with *Tg* values, that depend on storage conditions such as humidity and temperature. Amorphous materials with low moisture content and *Tg* values above storage temperature can be considered stable [43]. For this reason, glass transition temperatures for selected samples (12 and 16) and DPE were measured. The corresponding DSC thermograms are shown in Fig. 5. According to the half ΔCp method, the calculated glass transition temperatures were 117.1, 123.4, and 138.1 °C for the DPE, sample 12, and sample 16, respectively. Aerosil concentration increase allowed for improving *Tg* values and, consequently, enhancing product shelf life. The stability provided by Aerosil was also noticeable when the samples were conditioned at relatively high RH. In fact, for a relative humidity of 75% the DPE without carrier changed into a rubbery state, while samples 12 and 16 remained as powders.

4. Conclusions

According to the analysis of the results obtained in this work and comparison with those reported by other authors, it can be concluded that the optimal spray-drying operating conditions for a given plant extract/carrier system cannot be directly extrapolated from other formulations. Therefore, experimental work is unavoidable. Factorial design is a good alternative in order to identify, in a relatively fast and simple way, those combinations of spray-drying operating conditions that allow for the production of powders with good rheological properties and stability attributes.

High solids concentration, i.e. high carrier content, led to powders with good flowability properties and compactability — i.e. low angle of repose, low Carr's index, and acceptable hardness at low compression forces. Moreover, the use of high carrier concentrations significantly improved powder stability — low moisture content, low hygroscopicity, and high glass transition temperature.

Atomization air flow was also revealed to be a key operating condition. Low feed flow rates of atomizing air increased mean particle diameter, enhancing powder flowability. High solids concentrations also increased particle size. In fact, the higher the carrier content the higher the viscosity and surface tension of the dispersions and, consequently, the bigger the droplet sizes.

All the process yields obtained in the present work were very good for the mini spray dryer used. The best yields were found for high aspiration flow rates.

This work allowed to find operating conditions – e.g., tests 6 and 16 – to produce Cáscara sagrada extract powders that are adequate for direct compression and that have appropriate physical properties to ensure good product stability — i.e. a safe shelf life.

Acknowledgements

Authors express their gratitude for the financial support granted by the Consejo Nacional de Investigaciones Científicas y Técnicas (CONICET), the Agencia Nacional de Promoción Científica y Tecnológica (ANPCyT), the Universidad Nacional del Sur (UNS) and the Universidad Nacional de Córdoba of Argentina (UNC).

References

[1] D.S. Fabricant, N.R. Farnsworth, The value of plants used in traditional medicine for drug discovery, Environ. Health Perspect. Suppl. 109 (2001) 69–75.
[2] L. Bravo Díaz, Farmacognosia especial, first ed.Elsevier, Madrid, 2003.
[3] WHO, Monographs on Selected Medicinal Plants, 2, World Health Organization, Geneva, 2002.
[4] Y. Gonnissen, J.P. Remon, C. Vervaet, Development of directly compressible powders via co-spray drying, Eur. J. Pharm. Biopharm. 67 (2007) 220–226.
[5] H.A. Lieberman, L. Lachman, J.B. Schwartz, Pharmaceutical Dosage Forms: Tablets, second ed.Marcel Dekker, New York, 1990.
[6] C.A. Newall, L.A. Anderson, J.D. Phillipson, Herbal Medicines: A Guide for Health-Care Professionals, first ed.The Pharmaceutical Press, London, 1996.
[7] H.H. Tong, S.Y. Wong, M.W. Law, K.K. Chu, A.H. Chow, Anti-hygroscopic effect of dextrans in herbal formulations, Int. J. Pharm. 363 (2008) 99–105.
[8] Y. Gonnissen, S.I.V. Gonçalves, B.G. De Geest, J.P. Remon, C. Vervaet, Process design applied to optimize a directly compressible powder produced via a continuous manufacturing process, Eur. J. Pharm. Biopharm. 68 (2008) 760–770.
[9] C.R.F. Souza, W.P. Oliveira, Powder properties and system behavior during spray drying of *Bauhinia forficata* link extract, Drying Technol. 24 (2006) 735–749.
[10] S. Palma, R. Manzo, D. Allemandi, Dry plant extract loaded on fumed silica for direct compression: preparation and preformulation, Pharm. Dev. Technol. 4 (1999) 523–530.
[11] R.V. Tonon, C. Brabet, M.D. Hubinger, Influence of process conditions on the physicochemical properties of açai (*Euterpe oleraceae* Mart.) powder produced by spray drying, J. Food Eng. 88 (2008) 411–418.
[12] G.E.G. Moreira, M.G. Maia Costa, A.C. Rodrigues de Souza, E. Sousa de Brito, M.F. Dantas de Medeiros, H.M.C. Azeredo, Physical properties of spray dried acerola pomace extract as affected by temperature and drying AIDS, LWT Food Sci. Technol. 42 (2009) 641–645.
[13] T.P. Souza, R. Martínez-Pacheco, J.L. Gómez-Amoza, P.R. Petrovick, Eudragit E as excipient for production of granules and tablets from *Phyllanthus niruri* L spray-dried extract, AAPS Pharm. Sci. Tech. 8 (2007) E1–E7.
[14] L.A.L. Soares, G. González Ortega, P.R. Petrovick, P.C. Schmidt, Dry granulation and compression of spray-dried plant extracts, AAPS Pharm. Sci. Tech. 6 (2005) E359–E366.
[15] E.A.F. Vasconcelos, M.G.F. Medeiros, F.N. Raffin, T.F.A.L. Moura, Influência da temperatura de secagem e da concentração de Aerosil®200 nas características dos extratos secos por aspersão da *Schinus terebinthifolius* Raddi (Anacardiaceae), Braz. J. Pharmacogn. 15 (2005) 243–249.
[16] United States Pharmacopeia and National Formulary, USP 30–NF 25, The United States Pharmacopeial Convention, Rockville, MD, 2007.
[17] Real Farmacopea Española (RFE), Ministerio de Sanidad y Consumo, third edAgencia Española del Medicamento, Madrid, 2005.
[18] J. Barnes, L.A. Anderson, J.D. Phillipson, Herbal Medicines, third ed.Pharmaceutical Press, London, 2007.
[19] C. Kuklinski, Farmacognosia. Estudio de las drogas y sustancias medicamentosas de origen natural, first ed, Omega, Barcelona, 2003.
[20] J. Bruneton, Farmacognosia: fitoquímica: plantas medicinales, second ed.Acribia, Zaragoza, 2001.
[21] H. Wagner, S. Bladt, Plant Drug Analysis: A Thin Layer Chromatography Atlas, second ed.Springer-Verlag, Berlin, 1996.
[22] A. Schüssele, A. Bauer-Brandl, Note on the measurement of flowability according to the European Pharmacopoeia, Int. J. Pharm. 257 (2003) 301–304.
[23] A.L.R. Rattes, W.P. Oliveira, Spray drying conditions and encapsulating composition effects on formation and properties of sodium diclofenac microparticles, Powder Technol. 171 (2007) 7–14.
[24] A.K. Shrestha, T. Howes, B.P. Adhikari, B. Bhandari, Water sorption and glass transition properties of spray dried lactose hydrolyzed skim milk powder, LWT Food Sci. Technol. 40 (2007) 1593–1600.
[25] Mini Spray Dryer B-290, 29th October, 2010, http://www.buchi.com/Products.176.0.html.
[26] H. Takeuchi, S. Nagira, H. Yamamoto, Y. Kawashima, Solid dispersion particles of tolbutamide prepared with fine silica particles by the spray-drying method, Powder Technol. 141 (2004) 187–195.
[27] C. Bhaskar, S. Shimpi, A. Paradkar, Preparation and evaluation of glibenclamide-polyglycolized glycerides solid dispersions with silicon dioxide by spray drying technique, Eur. J. Pharm. Sci. 26 (2005) 219–230.
[28] S. Palma, C. Luján, J.M. Llabot, G. Barboza, R.H. Manzo, D.A. Allemandi, Design of Peumus boldus tablets by direct compression using a novel dry plant extract, Int. J. Pharm. 233 (2002) 191–198.
[29] R.C. Rowe, P.J. Sheskey, M.E. Quinn, Handbook of Pharmaceutical Excipients, sixth ed.Pharmaceutical Press, London, 2009.
[30] K. Ståhl, M. Claesson, P. Lilliehorn, H. Lindén, K. Bäckström, The effect of process variables on the degradation and physical properties of spray dried insulin intended for inhalation, Int. J. Pharm. 233 (2002) 227–237.
[31] L. Tajber, O.I. Corrigan, A.M. Healy, Spray drying of budesonide, formoterol fumarate and their composites — II. Statistical factorial design and in vitro deposition properties, Int. J. Pharm. 367 (2009) 86–96.
[32] M.J. Anderson, P.J. Whitcomb, DOE Simplified. Practical Tools for Effective Experimentation, second ed, Productivity Press, New York, 2007.

[33] M. Blumenthal, A. Goldberg, J. Brinkmann, Herbal Medicine: Expanded Commission E Monographs, Integrative Medicine Communications, Boston, 2000.
[34] ESCOP, European Scientific Co-operative of Phytotherapy Monographs, second ed, The Scientific Foundation for Herbal Medicinal Products, Exeter, 2003.
[35] J. Gruenwald, T. Bendler, C. Jaenicke, PDR for Herbal Medicines, third ed.Medical Economics Company, New Jersey, 2004.
[36] H.C. Ansel, N.G. Popovich, L.V. Allen, Pharmaceutical Dosage Forms and Drug Delivery Systems, ninth ed.Lippincott Williams & Wilkins, Philadelphia, 2009.
[37] A. Billon, B. Bataille, G. Cassanas, M. Jacob, Development of spray-dried acetaminophen microparticles using experimental designs, Int. J. Pharm. 203 (2000) 159–168.
[38] S.Y. Quek, N.K. Chok, P. Swedlund, The physicochemical properties of spray-dried watermelon powders, Chem. Eng. Process. 46 (2007) 386–392.
[39] http://www.buchi.com/Products.176.0.html. Process parameters Mini Spray Dryer B-290, 29th October, 2010.
[40] R.V. Tonon, C. Brabet, D. Pallet, P. Brat, M.D. Hubinger, Physicochemical and morphological characterization of açai (*Euterpe oleraceae* Mart.) powder produced with different carrier agents, Int. J. Food Sci. Tech. 44 (2009) 1950–1958.
[41] A. Dusanter, K. Saleh, P. Guigon, Formulation of highly concentrated suspensions for spray drying in a fluidized bed, KONA Powder Part. 26 (2008) 215–226.
[42] M. Cano-Chauca, P.C. Stringheta, A.M. Ramos, J. Cal-Vidal, Effect of the carriers on the microstructure of mango powder obtained by spray drying and its functional characterization, IFSET 6 (2005) 420–428.
[43] L.E. Kurozawa, K.J. Park, M.D. Hubinger, Effect of maltodextrin and gum arabic on water sorption and glass transition temperature of spray dried chicken meat hydrolysate protein, J. Food Eng. 91 (2009) 287–296.